Combined MAS NMR and X-ray Powder Diffraction Structural Characterization of Hydrofluorocarbon-134 Adsorbed on Zeolite NaY: Observation of Cation Migration and Strong Sorbate−Cation Interactions

Clare P. Grey,*,† Faiza I. Poshni,† Alessandro F. Gualtieri,‡ Poul Norby,†,§ Jonathan C. Hanson,§ and David R. Corbin⊥

Contribution from the Chemistry Department, SUNY Stony Brook, Stony Brook, New York 11794-3400, Dipartimento Scienze della Terra, Universitá di Modena, 41100 Modena, Italy, Chemistry Department, Brookhaven National Laboratory, Upton, New York 11973, and DuPont Central Research and Development (Contribution Number 7395), Wilmington, Delaware 19880-0262

Received October 14, 1996[⊗]

Abstract: ^{23}Na MAS NMR and synchrotron X-ray powder diffraction methods have been used to study the binding of hydrofluorocarbon-134 (HFC-134, CF_2HCF_2H) in zeolite NaY. A contraction of the volume of the unit cell is observed on gas adsorption, and the interaction of HFC-134 with the extraframework sodium cations is so strong that extraframework sodium cations in the sodalite cages (site I′) migrate into the supercages. These sodium cations are found on positions close to the site III′ positions of zeolite NaX. Both ends of the HFC molecules are bound to sodium cations, the HFC molecule bridging the site II and III′ cations in the supercages. The strong cation−HFC interaction results in a considerable displacement of the sodium site II cation along the [111] direction into the supercage and an increase in the T−O−T bond angle for the three oxygen atoms coordinated to this cation. A decrease in the ^{23}Na quadrupole coupling constant on HFC adsorption from 4.4 to less than 2.8 MHz, for the sodium cations originally located in the sodalite cages (site I′), is consistent with the sodium cation migrations.

Introduction

Chlorofluorocarbons (CFCs) have been linked to the seasonal ozone depletion over Antarctica, and consequently, the Montreal Protocol and later agreements have called for a complete phase out of chlorofluorocarbon production in developed countries by the year 2000.[1] Industry has identified several hydrofluorocarbons (HFCs) as possible CFC substitutes; however, the syntheses of the HFCs are much more complex than the syntheses of the CFC refrigerants and blowing agents[2,3] and involve many more steps. Unwanted HFC, hydrochlorofluorocarbon (HCFC), and CFC isomers are often produced during the reactions, and consequently, the purification of the products, and the removal of impurities, remains a concern. For example, in the synthesis of HFC-134a (CF_3CFH_2), the replacement for the refrigerant CFC-12 (CF_2Cl_2), the isomer HFC-134 (CF_2HCF_2H) is a common byproduct.[2,3] In addition, some of the impurities (e.g., CFC-114 (CF_3CFCl_2) and HCFC-124 ($CFClHCCF_3$)) have both ozone depletion and global warming potentials (ODP and GWPs). These factors have resulted in large increases in the cost for these new alternatives, over the original CFCs; this is partially responsible for the development of a CFC smuggling industry in the United States.[4] Basic zeolites have recently been found to be effective for separating various HFC mixtures,[5] which represents one approach for removing unwanted side products and improving product purity. The separation factor for the HFC-134/-134a mixture correlates with the Sanderson electronegativity[6] of the monovalent cation-exchanged forms of zeolite Y, increasing from Li, Na, K to CsY: the greater the electronegativity, the poorer the separation.[5]

We have been investigating the dehydrofluorination reactions of various HFCs over the basic X and Y zeolites and have recently published a gas chromatography (GC) and solid-state NMR study of the reaction of HFC-134 to form HFC-1123 (CF_2-CFH) over zeolite NaX.[7] The interactions with both the basic oxygen framework sites, and the extraframework (Lewis acid) sites have been shown to be important in controlling the reaction mechanisms and reactivity of many reactions over basic molecular sieves, for instance dehydrochlorination.[8] We have, therefore, been studying the adsorption of HFC-134a and HFC-134 on X and Y zeolites, with solid-state NMR and powder diffraction methods, to investigate the interactions of the HFCs with the extraframework and framework sites, and to determine how the HFC molecules are bound to the zeolite framework. These studies are also aimed at developing an understanding of the factors that are responsible for the gas separations.

† SUNY Stony Brook.
‡ Universitá di Modena.
§ Brookhaven National Laboratory.
⊥ DuPont Central Research and Development.
⊗ Abstract published in *Advance ACS Abstracts,* February 1, 1997.

(1) Molina, M. J.; Rowland, F. S. *Nature* **1974**, *249*, 810. Watson R. T.; Prather, M. J. Kurylo, M. J. *NASA Ref. Publ.* **1988**, No. 1208.
(2) Manzer, L. E. *Science* **1990**, *249*, 31. Manzer, L. E.; Rao, V. N. M. *Adv. Catal.*, **1993**, *39*, 329.
(3) Webb, G.; Winfield, J. *Chem. Brit.* **1992**, *28*, 996.
(4) See for example: *Chem. Eng. News* **1996**, *74* (Jan 15), 13. *New York Times,* September 1995.
(5) Corbin, D. R.; Mahler, B. A. World Patent, W.O. 94/02440, Feb 3, 1994.
(6) Sanderson, R. T. *Chemical bonds and bond energy,* 2nd ed.; Academic Press: New York, 1976.
(7) Grey, C. P.; Corbin, D. R. *J. Phys. Chem.* **1995**, *99*, 16821. Grey, C. P.; Corbin, D. R. *Stud. Surf. Sci. Catal.* (Weitkamp, J., Karge, H. G., Pfeifer, H., Hölderich, W., Eds.) **1995**, *98*, 89.
(8) Isao, M.; Czarny, Y. Z.; Oszczudlowski, J. *Pol. J. Appl. Chem.* **1991**, *3*, 187. Angell, C. L.; Howell, M. V. *J. Phys. Chem.* **1970**, *74*, 2737. Murray, D. K.; Chang, J.-W.; Haw, J. F. *J. Am. Chem. Soc.* **1993**, *115*, 4732. Murray, D. K.; Howard, T.; Goguen, P. W.; Krawietz, T. R.; Haw, J. F. *J. Am. Chem. Soc.* **1994**, *116*, 6354.
(9) Breck, D. W. *Zeolite molecular sieves*; John Wiley & Sons, Inc.: New York, 1974. Mortier, W. J. *Compilation of extraframework sites in zeolites*; Butterworth-Heineman: London, 1982.

S0002-7863(96)03565-2 CCC: $14.00

Three cation positions (sites I, I′, and II) are occupied in dehydrated zeolite NaY.[9] The site II cation position in the faujasite structure (zeolites X and Y) is located in the supercage and is coordinated to three oxygen atoms of the six-ring window to the sodalite cage, while the site I′ position is in the sodalite cage coordinated to three oxygen atoms of the double six rings. The ^{23}Na MAS NMR resonances of these cations are broadened by second-order quadrupolar interactions and give rise to overlapping resonances.[10] In contrast, cations in the site I position are in a more symmetric environment (D_{3d}) in the center of the double six-rings, resulting in a narrow resonance at approximately −11 ppm. Quadrupole coupling constants (QCC) of 4.8, 4.2, and approximately 0.1 MHz have been determined for sites I′, II, and I, respectively.[10] In a recent single-crystal structure refinement of dehydrated NaX, approximately 30 cations were observed in four site III′ positions.[11] These site III′ cations are located in the supercages and are coordinated to three oxygen atoms from three different four-rings. Cations in these positions also give rise to characteristic line shapes from which a quadrupole coupling constant of approximately 2.8 MHz has been extracted.[12]

We have published a preliminary report of the changes in the ^{23}Na MAS NMR of NaY and CsY, which occur on HFC-134 gas adsorption.[13] The ^{23}Na NMR data were consistent with a migration, on gas adsorption, of sodium cations originally located in the sodalite cages into the supercages. A diffraction study was, therefore, initiated in order to determine whether these cation relocations could be detected and to provide more detailed structural information on the HFC-134 binding. In this paper, we report the results of this combined ^{23}Na MAS NMR and X-ray diffraction study. Changes in the sodium local environment, as a function of HFC-134 loading level and temperature, are studied with NMR spectroscopy and the structures of NaY loaded with 32 and 16 molecules of HFC-134 per unit cell (uc) (i.e., four and two molecules per supercage, respectively) are determined with diffraction methods.

Experimental Section

Sample Preparation. Zeolite NaY was dehydrated under vacuum by slowly ramping the temperature of approximately 0.5 g of sample to 400 °C over a period of 6 h and holding at 400 °C for 16 h. HFC-134 (DuPont) was then adsorbed at room temperature at a variety of different loading levels. Loading levels were established by monitoring the drop of pressure, on exposure of the dehydrated sample to an atmosphere of HFC-134, with a carefully calibrated vacuum line and an absolute-pressure vacuum gauge. Samples are labeled *x*HFC-134/NaY, where *x* indicates the number of HFC molecules per unit cell. Samples were packed in a glovebox into zirconia rotors, and 0.3 mm quartz glass capillary tubes for the NMR and diffraction experiments, respectively. ICP elemental analysis of the original hydrated sample of NaY gave a composition (by weight percentage) of Na 6.94(4), Si 22.2(2), Al 8.26(6), leading to a composition of the unit cell of $Na_{52.8}Si_{138.4}Al_{53.6}O_{384}$.

NMR. Variable-temperature ^{23}Na MAS NMR experiments were performed with a double-tuned Chemagnetics probe, on a CMX-360 spectrometer. Small ^{23}Na flip angles were used (<15°) to ensure uniform excitation of the sodium nuclei with small and large quadrupole coupling constants. Chemical shifts are quoted relative to solid sodium chloride, as an external reference.

X-ray Powder Diffraction Data Reduction and Refinement. The X-ray powder diffraction experiments were performed at the X7B beamline at the National Synchrotron Light Source at Brookhaven Laboratory. This beamline is equipped with a four circle Huber diffractometer that holds a flat image plate detector (20 × 40 cm Fuji type).[14] Image plates (IPs) were scanned using a Fuji BAS2000 scanner. The wavelength for the data collection was determined with the standard LaB_6. The external standard was also used to determine the zero-shift position of the imaging plate, the sample to detector distance, and the tilting angle of the IP detector. The data reduction takes into account corrections for the Lorentz−polarization factor and the zero shift described by equations especially derived for the flat-plate IP geometry.[15] Data were collected at room temperature (RT) for bare NaY and at 100 K (LT) for bare NaY, 16HFC-134/NaY, and 32HFC-134/NaY with wavelengths and angular ranges (in 2θ) of 0.9445, 1.5585, 1.2726, and 0.9338 Å, and 5−55°, 2−120°, 2−55°, and 3−50° for bare NaY (RT and LT), 16HFC-134/NaY, and 32HFC-134/NaY, respectively. The NaY (LT) data were collected with a curved (INEL) 120° position sensitive detector. The maximum values for $\sin(\theta)/\lambda$ used (0.49, 0.56, 0.37, and 0.44, respectively) were comparable to the angular range used by Kaszkur et al. for the location of chloroform, dichlorobenzene, and 1,4-dibromobutane in zeolite Y.[16,17] No absorption correction was necessary, due to the chemical composition of the samples. Rietveld refinement of the data sets was performed with GSAS.[18] A total of 479, 502, 352, and 393 Bragg reflections were included in the refinements of bare NaY (RT and LT), 16HFC-134/NaY, and 32HFC-134/NaY, respectively. The 111 reflection could not be used in the data refinement of bare NaY (RT) due to a partial shadowing of this reflection by the beam stop, which resulted in a distorted intensity for this reflection. The intensity of this reflection was not affected by shadowing or by other instrumental aberrations in the data collected for NaY (LT), 16HFC-134/NaY, and 32HFC-134/NaY, and hence, the reflection could be included in the refinement. Four reflections in the low-temperature diffraction pattern of 32HFC-134/NaY (4.48°, 14.62°, 17.40°, and 26.07° in 2θ) could not be indexed with the faujasite unit cell (space group *Fd*3*m*). The reflections at 14.6° and 26.1° 2θ were attributed to ice. These reflections were not observed in the pattern of 16HFC-134/NaY. The very weak and broad reflection at 4.48 (<1%) is also present in that pattern 16HFC-134/NaY (at 6.02°), but not in that of bare NaY (RT), and is probably due to the low temperature setup. The lattice constants, phase fraction, and profile coefficients of the pseudo-Voigt function were refined initially. The diffraction peaks were modeled with a pseudo-Voigt function with three Gaussian and two Lorentzian line-broadening terms. The background curve was fit with a Chebyschev polynomial with a variable number of coefficients (16 for bare NaY and 24 for 16HFC-134/NaY and 32HFC-134/NaY). As a time-saving procedure, only a fixed number of background points were refined in the early cycles of the refinement.

Refinement Details. Early refinements were performed using the framework structure from the refinement by Fitch et al.[19] as a starting model. Difference Fourier maps were then calculated from the refined model and residual electron density from extraframework cations and adsorbed molecules was located. Repeated difference Fourier calculations were performed including cations and atoms extracted from the electron density maps. The intensity of especially the 111 reflection is very sensitive to the presence of extraframework molecules and ions. The calculated intensity of the 111 reflection for the framework alone is very high, and is dramatically reduced when adsorbing, e.g., HFC molecules in the zeolite. This results in severe problems in estimating the scale factor used to calculate the difference Fourier maps. It proved necessary to exclude the 111 reflection from the refinement, during the early stages of the refinement, for the refinements of the HFC-134/NaY data. However, it was very important to include this reflection

(10) Engelhardt, G.; Hunger, M.; Koller H.; Weitkamp, J. *Stud. Surf. Sci. Catal.* **1994**, *84*, 421. Hunger, M.; Engelhardt, G.; Koller H.; Weitkamp, J. *Solid State NMR* **1993**, *2*, 111.

(11) Olson, D. H. *Zeolites* **1995**, *15*, 439.

(12) Engelhardt, G.; Hunger, M.; Koller H.; Weitkamp, J. 11th International Zeolite Association Conference, Garmisch, August, 1994. Grey, C. P. Unpublished results.

(13) Grey, C. P.; Poshni, F. I.; Ba, Y; Corbin, D. R. *Mater. Res. Soc. Symp. Proc. (Microporous and Macroporous Materials)* **1996**, *431*, 177.

(14) Amemija, Y. *Synchrotron Radiation News* **1990**, *3*, 21.

(15) Norby, P. *J. Appl. Crystallogr.* **1997**, *30*, 21.

(16) Kaszkur, Z. A.; Jones, R. H.; Couves, J. H.; Waller, D.; Catlow, R. A.; Thomas, J. M. *J. Phys. Chem. Solids* **1991**, *52*, 1219.

(17) Kaszkur, Z. A.; Jones, R. H.; Waller, D.; Catlow, R. A.; Thomas, J. M. *J. Phys. Chem.* **1993**, *97*, 426.

(18) Larson, A. C.; Von Dreele, R. B. *GSAS. General Structure Analysis System*; Report LAUR 86-748; Los Alamos National Laboratory: New Mexico, 1995.

(19) Fitch, A. N. *J. Phys. Chem.* **1986**, *90*, 1311.

Table 1. The Agreement Factors Obtained for the Four Refinements

sample	NaY (RT)	NaY (LT)	16HFC-134/NaY	32HFC-134/NaY
R_P (%)[a]	2.2	2.0	2.3	3.8
R_{wP} (%)[b]	3.0	2.7	3.4	4.5
χ^2 [c]	9.9	8.1	25.5	25.7

[a] $R_P = \sum[Y_{io} - Y_{ic}]/[\sum Y_{io}]$. [b] $R_{wP} = [(\sum w_i*(Y_{io} - Y_{ic})^2) / \sum w_i Y_{io}^2]^{1/2}$. [c] $\chi^2 = [\sum w_i*(Y_{io} - Y_{ic})^2] / (N_{obs} - N_{var})$.

Table 2. The Fractional Coordinates, Occupancies (Occ), Temperature Factors (B), and Unit Cell Parameters (a_o) of the Framework Atoms and Sodium Cations for Dehydrated NaY (RT), Dehydrated NaY (LT), 16HFC-134/NaY, and 32HFC-134/NaY[a]

sites		NaY (RT)	NaY (LT)	16HFC/ NaY	32HFC/ NaY
T	x	−0.0538(1)	−0.0542(1)	−0.0540(2)	−0.0547(8)
(192i)	y	0.0360(1)	0.0358(1)	0.0372(8)	0.0366(1)
	z	0.1235(1)	0.1236(1)	0.1251(4)	0.1254(4)
	B	0.022(5)	0.021(8)	0.019(2)	0.019(1)
O(1)	$x = 0$				
(96h)	$y = -z$	−0.1071(2)	−0.1069(2)	−0.1078(1)	−0.1090(3)
	B	0.030(6)	0.021(8)	0.045(5)	0.016(1)
O(2)	$x = y$	−0.0023(3)	−0.0024(3)	−0.0018(1)	−0.0031(6)
(96g)	z	0.1437(3)	0.1436(3)	0.1424(5)	0.1413(4)
	B	0.026(5)	0.027(6)	0.007(7)	0.009(2)
O(3)	$x = y$	0.1763(2)	0.1762(2)	0.1816(2)	0.1800(9)
(96g)	z	−0.0349(3)	−0.0355(3)	−0.0346(8)	−0.0380(1)
	B	0.022(8)	0.009(6)	0.010(4)	0.011(3)
O(4)	$x = y$	0.1779(3)	0.1776(3)	0.1718(3)	0.1689(5)
(96g)	z	0.3193(4)	0.3192(3)	0.3238(1)	0.3235(4)
	B	0.035(6)	0.026(4)	0.046(3)	0.015(6)
Na(I)	$x = y = z = 0$				
(16c)	Occ	0.27(1)	0.270(9)	0.235(5)	0.24(3)
	B	0.034(2)	0.029(2)	0.011(5)	0.010(2)
Na(I′)	$x = y = z$	0.0551(3)	0.0550(3)		
(32e)	Occ	0.59(8)	0.598(11)	−	−
	B	0.022(4)	0.027(3)		
Na(II′)	$x = y = z$			0.1469(1)	0.1404(2)
(32e)	Occ	−	−	0.165(6)[c]	0.10(1)[c]
	B			0.036(6)	0.105(4)
Na(II)	$x = y = z$	0.2350(2)	0.2345(2)	0.2418(7)	0.2418(4)
(32e)	Occ	1[b]	1[b]	0.639(7)	0.67(2)
	B	0.058(2)	0.029(3)	0.011(9)	0.021(9)
Na(III′)	$x = y$			0.7146(4)	0.7176(4)
(96g)	z			0.4153(7)	0.4092(1)
	Occ	−	−	0.236(9)	0.29(6)
	B			0.061(4)	0.071(7)
a_o (Å)		24.7314(9)	24.6901(7)	24.6766(1)	24.6666(4)

[a] Occupancies are given for the sodium cations; all other sites are fully occupied. [b] The occupancy of this site refined to 100% very early on in the refinement and the occupancy was not refined in later stages of the refinement. [c] May include contribution from residual water molecules.

at a later stage of the refinements, for the same reason that it was necessary to exclude it in the early stage: i.e., it carries information concerning the extraframework ions and molecules.

Bare NaY. The structure of bare zeolite NaY was determined at room temperature and at 100 K. At both temperatures difference Fourier maps revealed the presence of sodium cations in sites I, I′, and II. (Nomenclature of extraframework positions as in ref 9). Refinement of the populations gave a total number of sodium ions of 55/uc, which is in good agreement with the chemical analysis. Agreement factors are listed in Table 1, refined atomic parameters in Table 2, and a plot of observed, calculated and difference profiles is shown in Figure 1a for the RT refinement.

32HFC-134/NaY. Refinement of the framework of 32HFC-134/NaY converged with $R_{wP} = 12.5\%$. A difference Fourier map revealed sodium ions populating sites I and II. Figure 2 shows a sections of

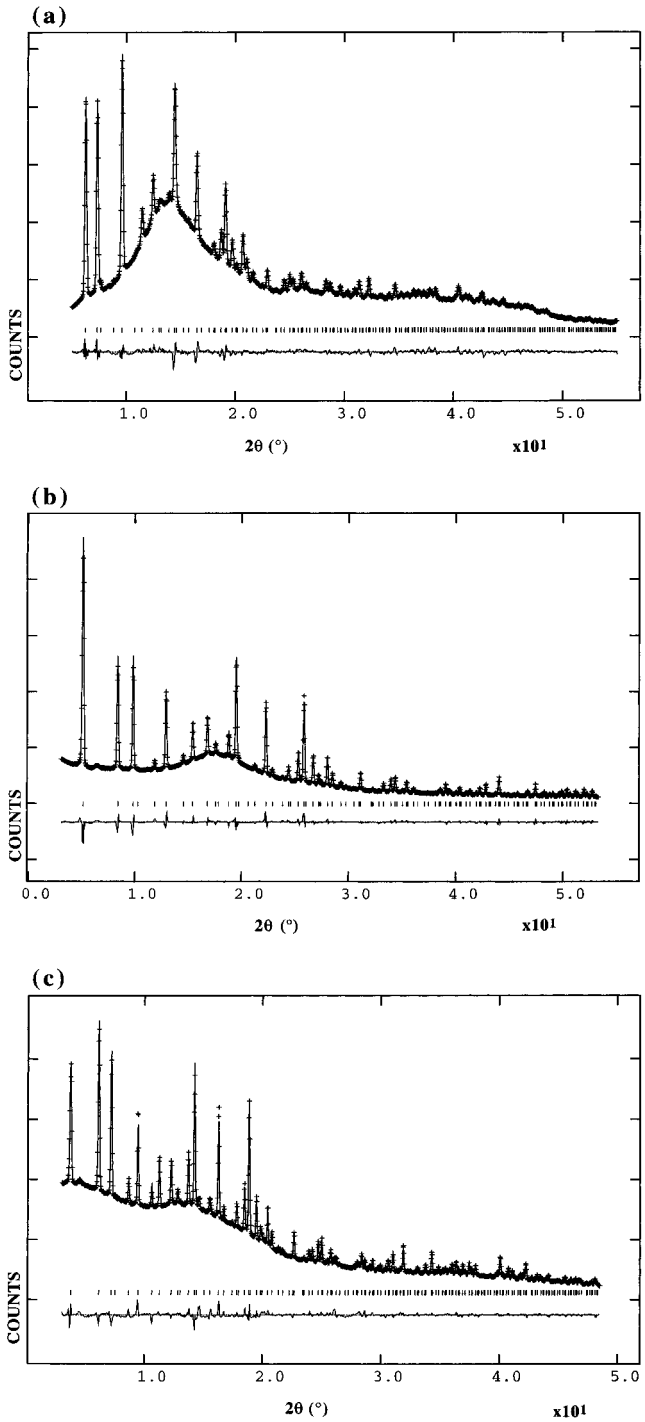

Figure 1. The observed (crosses), calculated (continuous line), and difference (bottom line) profiles of (a) bare NaY at room temperature, (b) 16HFC-134/NaY, and (c) 32HFC-134/NaY. Diffraction patterns are plotted in the range of 5−55°, 2−55°, and 3−50° 2θ for a, b, and c, respectively.

the difference Fourier map perpendicular to the [111] direction, computed after initial refinement of the (geometrically constrained) framework and sodium cations in sites I and II. The difference map reveals additional distributions of electron density with a center of gravity at approximately ($^3/_8$,$^1/_2$,$^3/_8$), which was attributed to the adsorbed molecules. The high number of symmetry-related, partially populated positions makes the interpretation of electron density maps of molecules adsorbed in zeolites with high symmetry structures a difficult task, when substantial disorder is present. Repeated difference Fourier maps were calculated, and gradually a model for the HFC-134 molecule was built up using a combination of information from the electron density map and chemical intuition. The model of the molecule contains two crystallographically distinct carbon atoms. Two localized fluorine

Table 3. The Fractional Coordinates, Occupancies (Occ), Temperature Factors (*B*) of Carbon and Fluorine Atoms Located in the Refinement of 16HFC-134/NaY and 32HFC-134/NaY

sites		16HFC/NaY	32HFC/NaY
C(1)	*x*	0.3723(3)	0.3703(9)
(192i)	*y*	0.4787(8)	0.4847(5)
	z	0.4149(6)	0.4109(3)
	Occ	0.162(8)	0.23(3)
	B	0.148(5)	0.148(5)
C(2)	$x = y$	0.3904(3)	0.3902(7)
(96g)	*z*	0.5364(5)	0.5407(5)
	Occ	0.324(8)	0.46(3)
	B	0.140(5)	0.147(3)
F(1)	$x = y$	0.4282(1)	0.4275(3)
(96g)	*z*	0.5535(5)	0.5571(9)
	Occ	0.324(8)	0.46(3)
	B	0.167(7)	0.120(5)
F(2)	*x*	0.3411(5)	0.3412(7)
(192i)	*y*	0.5619(2)	0.5673(4)
	z	0.4028(1)	0.3978(4)
	Occ	0.162(8)	0.23(3)
	B	0.151(4)	0.065(8)
F(3)	*x*	0.4064(1)	0.4068(3)
(192i)	*y*	0.4741(7)	0.4691(1)
	z	0.4602(2)	0.4507(4)
	Occ	0.162(8)	0.23(3)
	B	0.124(6)	0.138(8)
F(4)	$x = y$	−0.1811(5)	−0.1807(6)
(96g)	*z*	0.2567(9)	0.2467(7)
	Occ	0.324(8)	0.46(3)
	B	0.158(4)	0.156(7)

atoms were found around each carbon: C(2) is bound to F(1) and F(2), and C(1) is bound to F(4) and F(3) atoms.

From the refinements and the calculated difference Fourier maps it was clear that additional sodium positions were populated. A position close to that of the site III′ position found in zeolite NaX was interpreted as sodium cations (see Figure 2b). This position is very close to one of the fluorine atoms (F(1)), but both positions are only partially occupied. The refinements also revealed that the site I′ was no longer populated, while site II′ became partially populated. Interactions (i.e., short interatomic distances) between Na(II) and F(2), and between Na(III′) and F(2) and F(3) were found. Final refinements were performed with soft constraints on the C−F and C−C distances and the C−C−F angles. The relative populations of the C's and F's were restrained to preserve the stoichiometry of the molecule. Positions, populations, and thermal parameters were refined. The high symmetry results in severe overlap of the symmetry related atoms, and it was not possible to release the geometric constraints of the molecule during the refinement. The refinement converged with *R* values as given in Table 1. Refined positions of the framework and extraframework cations are given in Table 2 and of the adsorbed molecules in Table 3. Figure 1b shows the observed, calculated, and difference powder diffraction profiles. Superimposed on the difference Fourier map of Figure 2 are the positions of the refined atoms in the HFC molecules and sodium cations in site III′. The final positions of the HFC-134 molecule generally fit the electron density found in the initial difference Fourier map, but some discrepancies are observed. A similar observation was reported by, e.g., Kaszkur et al. when locating chloroform and dichlorobenzene in zeolite NaY.[16] There may be a number of reasons for these discrepancies. First, the calculated phases in the Fourier computation may be wrong, because of the substantial contribution to the diffraction from the extra framework species; this will result in errors in the difference maps. Second, the molecules are likely to be disordered in the zeolite cages: while the model found refines satisfactorily and makes chemical sense, it probably describes favored or average positions of the molecules. The total number of sodium ions determined from the refinement is 56 Na/uc, which is in good agreement with the expected number. However, the total number of HFC-134 molecules refines to 44 molecules per unit cell, i.e., 5.5 molecules per supercage. This should be compared to the expected value of 32 molecules per unit cell, or 4 molecules per supercage. This discrepancy is most likely due to the positional disorder of the molecules.

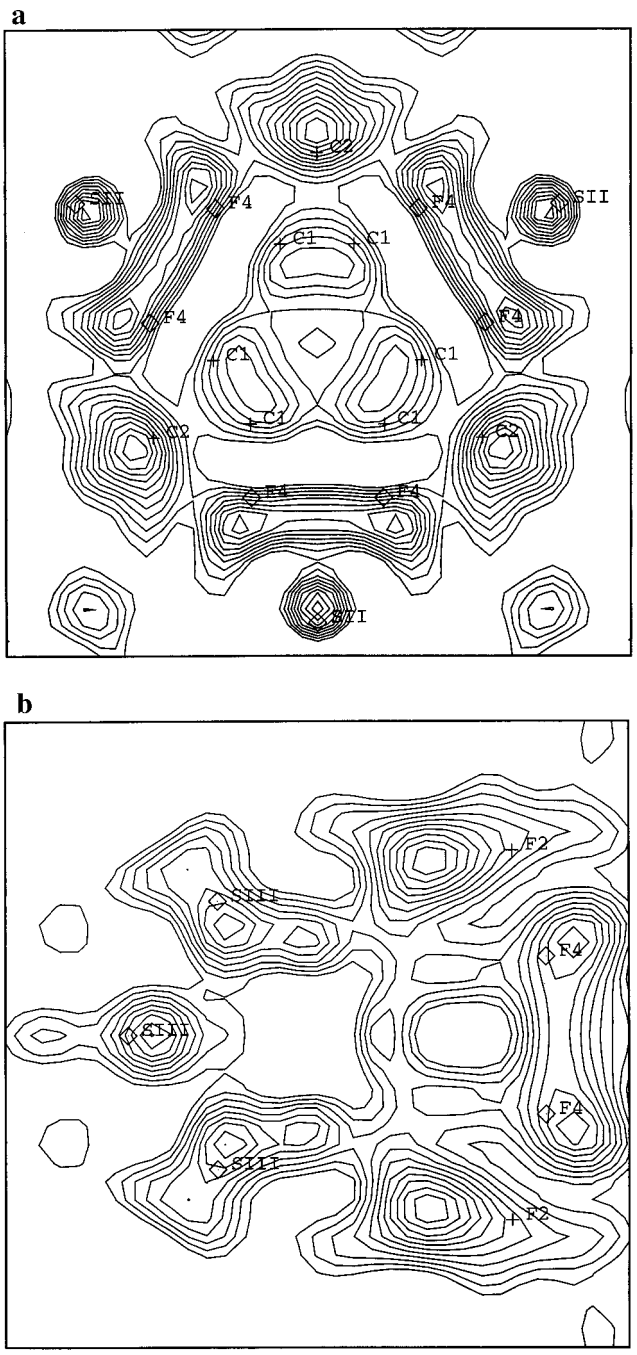

Figure 2. Sections of the difference Fourier map, perpendicular to the [111] direction and centered at (a) (0.42,0.42,0.42) and (b) (0.782,0.775,0.476). Difference Fourier maps were calculated after the initial refinement of the zeolite framework (see text). Final, refined atomic positions of the cations and HFC molecules are indicated. Map sizes of (a) 12 × 12 and (b) 10 × 10 Å^2 are shown.

16HFC-134/NaY. The refinement of the powder diffraction data for 16HFC-134/NaY, with only the framework positions, converged easily with an R_{wP} of 10.7%. Again, difference Fourier maps were calculated and electron density that was attributed to the adsorbed molecules was found in approximately the same position as for the higher loading sample. Computation of successive difference Fourier maps allowed a model to be built up, which was very close to that found for the 32HFC-134/NaY sample. Rietveld refinement with constraints similar to those for the higher loading sample converged with $R_{wP} = 4.5\%$. The position of the molecule and the distribution of the sodium ions were similar to the previous sample. Again, the total population of the cations (52 Na/uc) is in good agreement with

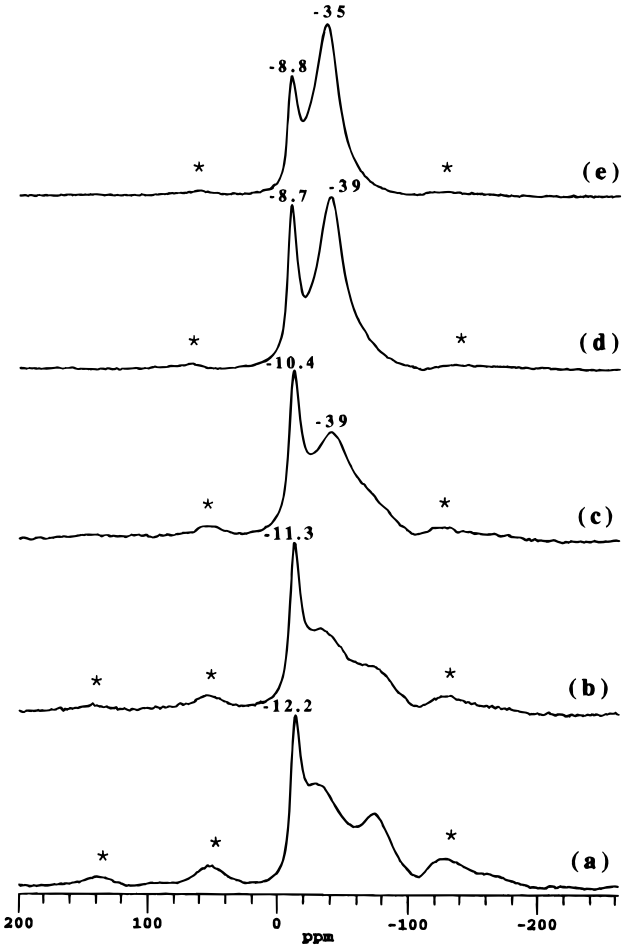

Figure 3. The ^{23}Na room temperature MAS NMR spectra of *x*HFC-134/NaY, for $x = 0$ (a), 4 (b), 16 (c), 32 (d), and excess (e), where value of *x* indicates the number of HFC-134 molecules per unit cell. Spectra were obtained with spinning speeds of 7−10 kHz. The discontinuities in the second-order quadrupolar broadened line shapes from the cations in the sodalite and supercages are marked on spectra c−e. Chemical shifts of the resonances from site I cations (−8.8 to −12.2 ppm) are also indicated. Spinning sidebands are indicated with asterisks.

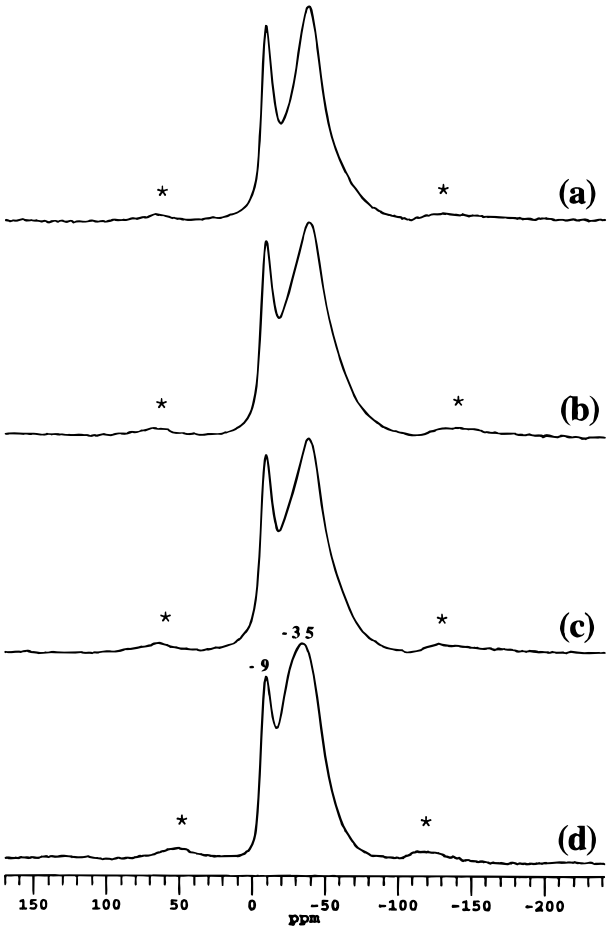

Figure 4. The ^{23}Na variable-temperature MAS NMR spectra of 32HFC-134/NaY at (a) room temperature, (b) −50, (c) −100, and (d) −150 °C. Spinning speeds of 8.3−8.7 kHz were used. (Spinning sidebands are indicated with asterisks; the shift (site I) and discontinuity of the resonances are marked for the spectrum obtained at −150 °C.)

the expected value, while the population of the adsorbed molecules is higher than expected.

Results

^{23}Na NMR. Figure 3 shows the effect of HFC-134 loading level on the room temperature ^{23}Na MAS NMR spectra of NaY. The spectrum of dehydrated NaY is similar to previously reported spectra:[10] the narrow resonance at −12 ppm is assigned to the site I cations, and the broader resonance spreading from approximately −15 to −120 ppm contains two overlapping resonances from sodium nuclei in the site II and I′ positions. On adsorption of HFC-134, the resonances from the cations originally in sites I′ and II narrow considerably and a resonance centered at approximately −39 ppm grows in as the loading level is increased. At lower loadings, the broader resonances from the bare I′ and II cations are still visible as shoulders to low frequency of the discontinuity at −39 ppm. At high loading levels, these signals can no longer be detected within the limits of sensitivity of the experiment. In contrast, the line width of the resonance from the site I cations remains unaffected, but the chemical shift of this resonance moves to higher frequencies with increased gas loading. The narrowing of the line width of the resonances from the cations originally in the site II and I′ positions, is due to a reduction of the QCC, and thus the second-order quadrupolar broadening, for these nuclei. Spectra were obtained as a function of temperature for 32HFC-134/NaY (Figure 4) so as to exclude any possibility that the reduction of the sodium QCC results from an increase in cation mobility. Small changes in the line shapes were observed with temperature, the resonance initially centered at −39 ppm broadening with decreasing temperatures, and shifting to approximately −35 ppm. These changes appear consistent with a change in the asymmetry parameter, η, but not a significant change in the QCC. Even at the lowest temperature, the second-order quadrupolar broadenings are much smaller than those observed for the site II and I′ cations in bare NaY.[10] The variable temperature spectra of 16HFC-134/NaY (Figure 5) also show significant changes as the temperature is decreased. The intensity of the low-frequency shoulder of the resonance at −39 ppm, which was ascribed to a bare cation site, decreases and at −150 °C is no longer discernible.

A reduction in the QCC of the cations originally in sites I′ and II, on HFC adsorption, indicates that these cations are now in more symmetric and possibly higher coordination environments. The reduction of the QCCs from the site I′ cations is, however, extremely surprising. HFC-134 molecules cannot enter the small sodalite cages, so binding to the sodalite cage sites is not a possibility. On the basis of these NMR results we, therefore, propose that the site I′ cations migrate out of these sites and into the supercage, where they can interact with the HFC molecules; this will result in the experimentally observed reduction in the QCC for the cations originally in both

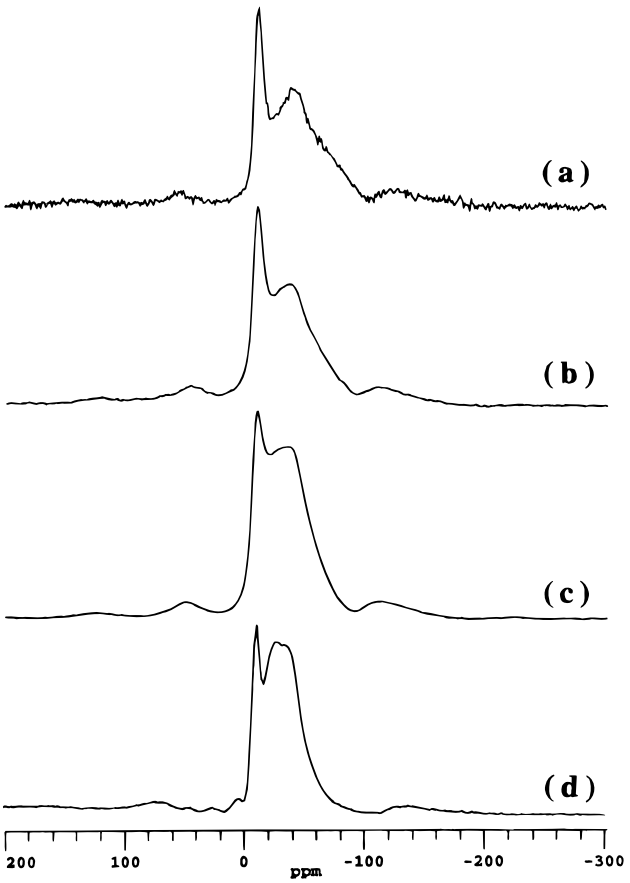

Figure 5. The ^{23}Na variable-temperature MAS NMR spectra of 16HFC-134/NaY at (a) room temperature, (b) −50, (c) −100, and (d) −150 °C. Spinning speeds of 7.0−7.4 kHz were used.

the site I′ and II cation positions. The change, with temperature, in the ^{23}Na QCCs of the sodium cations originally in the I′ and II sites, is consistent with Na-HFC interactions. As the temperature decreases, the mobility of the HFC is reduced, altering the electric field gradient at the sodium sites. Furthermore, the low-temperature spectra of 16HFC-134/NaY indicate that loading levels of as low as 16HFC/uc result in migration of the site I′ cations.

We were only able to acquire ^{23}Na MAS spectra at one magnetic field strength. Hence, it is difficult to separate the contributions from the second-order quadrupolar shift and chemical shifts (δ_{iso}) to the MAS resonances, and thus to perform detailed simulations to extract values for the QCC, η, and δ_{iso}. The line shapes for the resonance centered around −35 to −39 ppm are not consistent with a single sodium QCC and η, and a number of different local environments are present. However, to provide approximate estimates of the magnitude of the decrease of the QCC with gas loading, we performed simulations of the different line shapes, using a variety of different values for the QCC, η, and δ_{iso}. These simulations place upper limits on the size of the QCCs, and it is important to stress that the inclusion of different sites with differing δ_{iso}, may result in smaller values for the QCC. Reasonable fits were obtained with QCCs of approximately 2.8 MHz for the resonance centered at −39 ppm in the room temperature ^{23}Na spectrum. The spectrum of the ^{23}Na cations contributing to the resonance at approximately at −150 °C was fit by including a larger value for the Gaussian line broadening (Figure 6). This may be indicative of a greater range of ^{23}Na local environments at low temperatures. The estimates for the QCCs are very close to that obtained for site III′ cations in bare NaX.[12] The site II cation positions are fully, or close to fully, occupied in bare

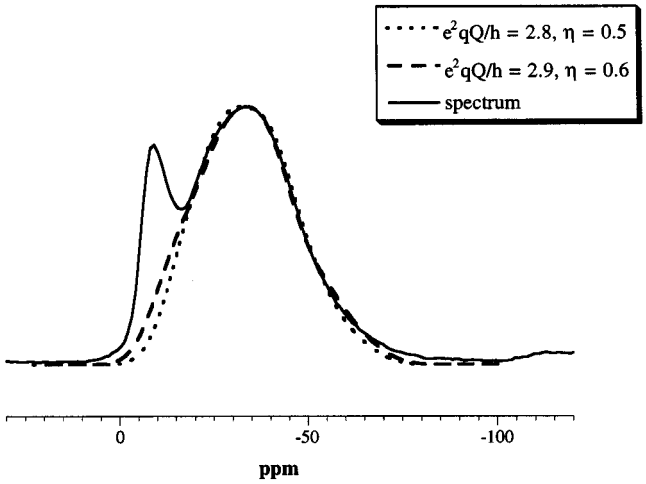

Figure 6. An example of the simulations of the ^{23}Na second-order quadrupolar line shapes used to extract approximate values for the QCC and η for the resonances centered at −35 to −39 ppm (see text). Gaussian broadening = 1200 Hz, QCC = 2.8 MHz, η = 0.5, δ_{iso} = −11 ppm, and QCC = 2.9 MHz, η = 0.5, δ_{iso} = −8 ppm, were used for the two fits of the one pulse spectrum of 32HFC-134/NaY collected at −150 °C.

NaY, thus any cations that migrate from the sodalite cages must occupy new sites. The most plausible location for these cations is in the site III′ position; this suggestion is consistent with the QCCs obtained for these cations.

Diffraction. The framework and cation positions for all four structures are reported in Table 2. The structure of bare NaY is consistent with that obtained from earlier diffraction studies.[19,20] A total of 4, 19, and 32 sodium cations/uc were found in the three cation positions along the 3-fold axis (sites I, I′, and II), corresponding to site occupancies of 27, 60, and 100%, respectively. These occupancies are similar to those obtained by Fitch et al.[19] from neutron diffraction studies (7.1, 18.6, and 32.8 cations/uc) except for the Na(I) site, which is slightly less populated. A small but significant decrease in the unit cell parameter, a_o, occurs on gas adsorption, and the unit cell is smallest for the highest HFC loading level. The occupancy of the site I cation position (7%) is essentially unchanged on gas adsorption. In contrast, significant changes in the cation locations and occupancies were observed for the other cation positions. The occupancy of the site I′ in the sodalite cages refines to zero even for the 16HFC-134/NaY samples. Approximately 5.3 and 3.2/uc of these cations migrate to the site II′ position, which is also located in the sodalite cages, in the 16HFC and 32HFC-134/NaY samples, respectively. The occupancy of the site II position, which is on the other side of the six-ring window from the site II′ position and cannot be simultaneously occupied, decreases to 20 and 21/uc for 16HFC and 32HFC-134/NaY samples, respectively. The most dramatic change, however, is the high occupancies (23 and 28/uc for 16HFC and 32HFC-134/NaY, respectively) found for a Na(III′) site, which is close to the III′ sites found in NaX.[12] Unlike the single-crystal study of bare NaX, however, we only refined one independent Na(III′) position.

Selected bond distances and angles for the framework and cation positions are reported in Table 4. A significant increase in the Na(II)−O bond lengths is observed on HFC loading for both the three closest oxygen atoms (O(2)), and the more distant O(4) atoms, increasing from 2.34 to 2.48 and 2.51 Å for Na(II)−O(2) on adsorbing 16 and 32 HFC molecules/uc, respec-

(20) Eulenberger, G. R.; Shoemaker D. P.; Keil, J. G. *J. Phys. Chem.* **1967**, *71*, 1812.

Table 4. Selected Bond Lengths and Angles for the Framework and Cationic Sites for RT and LT Dehydrated NaY, 16HFC-134/NaY and 32HFC-134/NaY[a]

	NaY (RT)	NaY (LT)	16HFC/NaY	32HFC/NaY
T−O(1)	1.643(5)	1.631(4)	1.670(12)	1.665(17)
T−O(2)	1.666(5)	1.668(4)	1.664(13)	1.653(21)
T−O(3)	1.613(4)	1.617(3)	1.667(14)	1.648(24)
T−O(4)	1.658(5)	1.657(4)	1.610(16)	1.604(15)
Na(I)−O(3)	2.716(8) × 6	2.727(7) × 6	2.535(8) × 6	2.616(21) × 6
Na(I′)−O(2)	2.975(1) × 3	2.975(9) × 3		
Na(I′)−O(3)	2.318(8) × 3	2.334(7) × 3		
Na(II)−O(2)	2.337(8) × 3	2.336(7) × 3	2.478(21) × 3	2.510(14) × 3
Na(II)−O(4)	2.888(9) × 3	2.892(8) × 3	3.172(18) × 3	3.245(15) × 3
Na(III′)−O(1)			3.118(12) × 2	3.057(12) × 2
Na(III′)−O(4)			2.707(16)	2.712(13)
O(1)−T−O(2)	112.1(5)	112.4(4)	111.3(11)	110.8(5)
O(1)−T−O(3)	111.0(5)	110.6(4)	105.5(7)	105.7(9)
O(1)−T−O(4)	107.8(5)	108.8(4)	106.7(3)	107.5(11)
O(2)−T−O(3)	109.7(5)	109.7(4)	105.1(8)	107.5(11)
O(2)−T−O(4)	103.9(6)	104.0(5)	114.5(7)	118.0(9)
O(3)−T−O(4)	112.2(6)	111.1(5)	113.4(12)	106.5(9)
T−O(1)−T	133.6(7)	134.4(6)	135.2(5)	133.2(7)
T−O(2)−T	141.5(7)	141.5(6)	146.1(10)	148.9(9)
T−O(3)−T	142.7(7)	143.5(6)	133.8(11)	140.1(12)
T−O(4)−T	144.9(8)	146.4(6)	143.9(4)	146.4(12)

[a] Distances are in Angstroms and angles are in degrees.

Table 5. Selected Bond Lengths for the Cations and HFC-134 Molecules in 16HFC-134/NaY and 32HFC-134/NaY[a]

	16HFC/NaY	32HFC/NaY
Na(II)−F(4)	2.72(2)	2.71(2)
Na(III′)−F(1)	2.70(1)	2.70(1)
Na(III′)−F(2)	3.26(1)	3.25(2)
Na(III′)−F(3)	3.09(2)	3.38(1)
C(1)−C(2)	1.57(2)*	1.55(2)*
C(1)−F(3)	1.40(2)*	1.39(2)*
C(1)−F(4)	1.42(2)*	1.43(2)*
C(2)−F(1)	1.38(1)*	1.36(2)*
C(2)−F(2)	1.40(1)*	1.39(2)*

[a] Distances are in Angstroms. Distances marked with asterisks were refined with soft constraints.

tively. The increase in interatomic distances also results in changes in the T−O(2)−T angles, altering from 141.5° (NaY) to 146.1° (16HFC) and 148.9° (32HFC). A flattening of the O(2)−T−O(4) angle is also seen on HFC adsorption. These results should be contrasted with benzene adsorption where only very small changes in the Na(II)−O(2) bond lengths were observed (2.35 to 2.40 Å)[19] and much smaller changes in framework bond angles occurred.

The Na(III′)-O distances observed in our refinement of approximately 2.71 Å (Na(III′)−O(4)) and 3.06 Å (×2) (Na(III′)−O(1)) are considerably longer than those for the most symmetric site III′ cation position observed in NaX [2.22 Å (O(4)); 2.81 and 2.85 Å (O(1))], but are only slightly longer than the average Na−O distances found for the other two III′ sites (2.75 and 2.88 Å).[11] Given the large lengthening of the Na(II)−O distances observed on HFC adsorption and the lower charge of the Y framework (in comparison to X), the Na(III′)−O distances do not appear unreasonable for a sodium cation that is also bound to an HFC molecule. The 3-fold axes generate three positions for the Na(III′) atoms which are in very close proximity to each other (2.6 Å) and cannot be simultaneously occupied; this is clearly possible, due to the low occupancy of the site.

The atomic positions and selected bond distances of the HFC-134 molecules are reported in Tables 3 and 5. Two carbon atoms were used in our model to fit the electron density seen in the Fourier difference maps. One carbon atom C(2) lies on

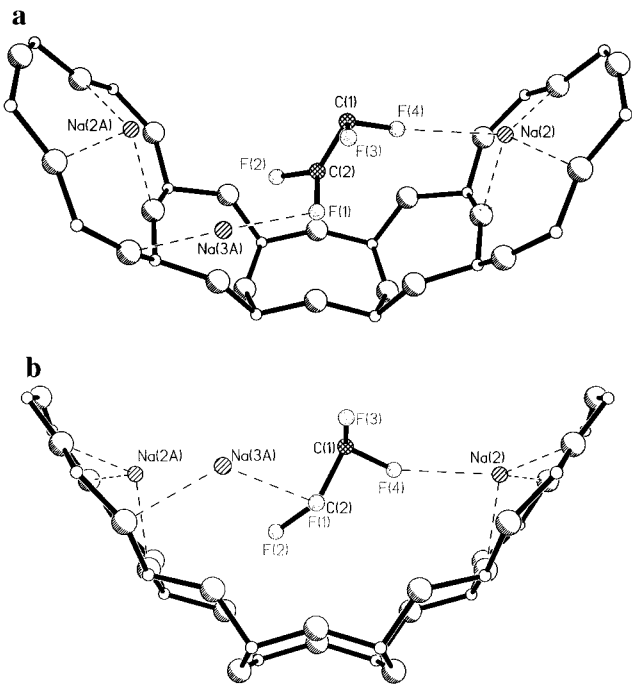

Figure 7. The HFC-134 molecules bound to the framework of zeolite NaY. The plots were generated utilizing the refined C and F atomic positions. The short Na(III′)−F(1) and Na(II)−F(4) contacts are shown with dashed lines. (Na(III′) is indicated as Na(3a).) Short Na(III′)−O(4) and Na(II)−O(2) distances are also indicated. Two different orientations are shown. The view down one {110} mirror plane is shown in b, so that the atoms that lie on this symmetry element are more clearly discernible.

the (110) mirror plane on a 96-fold position while C(1) is on a lower symmetry site (a 192-fold position), lying slightly off the mirror planes. The mirror plane generates two symmetry-related C(1) sites that are only separated by 1.55 Å and cannot be occupied simultaneously. Thus the molecule is disordered and is statistically distributed across the mirror plane. The C(2) carbon atom is coordinated to three (partially occupied) fluoride ion sites, where one fluorine atom F(1) is located on the (110) mirror plane and the other two fluorine atoms (F(2)) are symmetry related by the mirror plane. C(1) is coordinated to one F(3) and one F(4) atom.

The high symmetry of the system generates many different C, F, and Na(III′) positions which cannot all be simultaneously occupied. Each HFC molecule is close to three possible Na(III′) sites, and three different arrangements of the HFC molecule, in relation to these Na(III′) sites can be generated. The first is excluded due to a short Na(III′)−F(1) (1.63 Å) distance and consequently both positions cannot be simultaneously occupied. However, the F(1) sites are at reasonable distances from two other Na(III′) cations (2.6 Å). Figure 7a shows one of the two possible coordination environments for the HFC molecules. Two of the six-rings of the Si−O−Si(Al) framework, which are separated by three fused four rings, are shown. The 3-fold symmetry axis at the center of the six ring generates a tetrahedral arrangement of six rings which, with the four rings, form the supercage of the faujasite structure. The HFC-134 molecule lies across one of the four-rings and is bound at both ends to sodium cations. The F(4) atom, bound to C(1), is located only approximately 2.7 Å from Na(II) and is coordinated to this cation. Na(III′) is also near to the F(1) and F(2) atoms (2.7 and 3.3 Å, respectively) that are coordinated to C(2) and bridges the other end of the HFC molecule to the framework. Figure 7b shows the same HFC/Na arrangement as in 7a, but with a different orientation. C(2) is now located

behind F(1) and the (110) mirror plane that runs though C(2) and F(1) and O(4) is now clearly visible. Although the environment shown in Figure 7 appears to be the most plausible and realistic binding arrangement, another configuration may be possible. This can be generated from the same cation arrangement shown in Figure 7a and b by utilizing the second C(1) atom coordinated to C(2). The (110) mirror plane through C(2) and F(1) generates the second C(1) position, and the HFC molecule now points toward Na(III′). However, a short Na-(III′) to F(3) distance is generated (2.40 and 2.55 Å, for 16- and 32HFC structures, respectively), suggesting that this coordination environment may be less energetically favorable. In addition, both ends of the molecule are more effectively bound in the sodium coordination shown in Figure 7a and b. In the higher loaded sample, the refined population of the Na(III′) atoms (ca. 28) is comparable to the number of expected HFC molecules/uc, whereas the refined populations of the Na(II) atoms (ca. 22) are somewhat lower. Thus, approximately 70% of the molecules are bound at both ends to the framework via sodium cations. In contrast, the refined population of the Na-(III′) and Na(II) cations is comparable to the number of HFC-134 molecules/uc for the lower loaded sample, and the molecules appear to be bound on either side to the framework via the cations. These structures appear to represent reasonable models for HFC binding. In practice, considerable disorder is present and a number of such structures will be present. In addition, small numbers of alternative HFC/sodium cation arrangements may exist that we were unable to detect in our refinements.

Discussion

The X-ray powder diffraction of 32HFC-134/NaY showed considerable disorder in the location of the HFC-134 molecules. There are a number of possible reasons for this. First, the rotation of the CF_2H group about the C−C axis will cause positional disorder of the F atoms. Second, there may be more than one HFC conformer present: the presence of both the trans and the staggered-gauche conformers of HFC-134 adsorbed on NaX has been suggested from Raman experiments.[21] Finally, disorder in the number of sodium atoms coordinated to the HFC-134 molecule will almost certainly result in a distribution of HFC-134 binding sites. The temperature factors associated with the HFC molecules are higher than those of the framework and sodium cations, and the electron density of the different fluorine atom sites overlaps; again, this is most likely a consequence of the HFC disorder, but may also be due to residual HFC motion. The disorder, and the constraints imposed on the fluorine atoms, clearly affects the population of the carbon atom sites, and is likely to be a cause of the discrepancy between the HFC occupancies obtained from the refinements and those determined during the gas loading experiments. It is important to emphasize that the HFC binding arrangement that we have chosen to model the electron density accounts for all the major electron-density peaks in the Fourier maps and generates chemically reasonable binding environments for the HFC molecules. In addition, the cation distributions are consistent with those observed in the ^{23}Na MAS NMR. However, we cannot totally exclude the possibility that other binding arrangements may be present which are obscured by the high-symmetry space group of the faujasite structure and the low symmetry of the adsorbate.

It was not possible to locate all the sodium cations, unless the 111 reflection was included in the refinement of 32HFC-134/NaY. This reflection contains low resolution structural information concerning supercage structure, particularly for the cations located along the ⟨111⟩ directions. It is often common practice, however, to omit this reflection from the Rietveld refinements of loaded faujasite samples, due to the large errors that can occur at small angles. This work suggests that this omission may result in a loss of structural information.

The combination of the ^{23}Na NMR and diffraction data provide convincing evidence that considerable sodium cation migrations occur on HFC-134 adsorption. The HFC/Na(II) interactions are also responsible for a significant displacement of the Na(II) cations into the supercages. Both the low-temperature ^{23}Na NMR and the diffraction studies of 16HFC-134/NaY show a disappearance of the site I′ cation site. The very small shoulder to lower frequencies which is barely visible on the low-temperature ^{23}Na spectra of both 16 and 32HFC-134/NaY may be due to the small concentration of cations in the site II′ positions that were refined in the diffraction data.

The interaction of the fluorine atoms of CF_2HCF_2H with the sodium cations is apparently sufficiently large that the less favorable arrangement of sodium cations (site II + III′) for the bare Y zeolite results in the lower energy structure on HFC loading. The site III or III′ positions are, however, occupied by cesium cations in dehydrated (bare) CsY.[22] Coordination to two sodium cations clearly maximizes the interactions with the partial negative charges (of the fluorine atoms) that are located at either end of the HFC-134 molecule. This arrangement also allows an interaction of the HFC molecule with the zeolite framework, although the shortest F to O and C to O distances are 3.0 and 3.6 Å, respectively. On average, approximately 30% of the HFC molecules in 32HFC-134/NaY are only bound to a single cation (Na(III′)). The Na(III′) cations may be bound, however, to more than one HFC molecule. This arrangement may maximize Na−F interactions at higher loadings and may help explain the decrease in Na(II) occupancy: HFC−Na(III′) binding may be more energetically favorable than HFC−Na(II) binding, since the number of Na−F contacts are maximized. Further structural refinements, as a function of loading level and temperature, are in progress to explore these postulates further.

The coordination of the HFC-134 molecule to both the SII and SIII′ cations suggests an explanation for the very strong binding of HFC-134 observed over NaX zeolites: These sites are already occupied in NaX, and no large structural rearrangements are required to maximize the Na−F interactions. The arrangement observed for the HFC binding in NaY, may offer an explanation for the occurrence of the dehydrofluorination reaction of HFC-134 in NaX at moderate temperatures (∼250 °C). This reaction also occurs for HFC-134 in NaY at higher temperatures. The $H-O_{framework}$ and F−Na interactions are likely to be important in lowering the activation energy for this reaction, the F−Na interaction stabilizing the poor fluoride ion leaving group. Both these interactions can be maximized in this binding arrangement.

Cation migrations into the supercages were not observed in earlier structural refinements for the adsorption of chloroform, dichlorobenzene, and 1,4-dibromobutane in NaY.[16,17] Chloroform molecules were located near the four rings that bridge the two sodalite cages and short Cl−O(4) and Cl−O(1) distances

(21) Udovic, T. J.; Nicol, J. M.; Cavanagh, R. R.; Rush, J. J.; Crawford, M. K.; Grey C. P.; Corbin, D. R. *Mater. Res. Soc. Symp. Proc.* **1995**, *376*, 751.

(22) Godber, J.; Baker, M. D.; Ozin, G. A. *J. Phys. Chem.* **1989**, *93*, 1409. Lai, P. P.; Rees, L. V. C. *J. Chem. Soc., Faraday Trans.* **1976**, *72*, 1809. Poshni, F. I.; Ba, Y.; Ciraolo, M. F.; Grey, C. P.; Gualtieri, A.; Norby, P.; Hanson, J. C. Unpublished results.

of less than 3 Å were observed.[16] A decrease in the Na(II)occupancy with high loading levels was also observed, and it was suggested that this was due to a repulsion between the chloroform molecules and the cations. In contrast, the bromine atoms of dibromobutane were observed to coordinate to the Na(II) cations, and interaction with the cation site I′ positions was proposed (from molecular dynamics simulations) to account for a second adsorption site.[17] Sodium ion migrations from the sodalite cages have been observed on adsorption of more polar molecules. The most obvious example is the case of water adsorption, where cation migration to a variety of sites including Na(III) has been observed.[23] Water adsorption also results in a contraction of the unit cell parameters (by approximately 0.02[24] to 0.1 Å[23]). A variety of cation sites in the supercages are occupied on adsorption of polar aromatics such as m-nitroaniline and m-dinitrobenzene in NaY.[25,26] The Na(III′) (and II*) sites are occupied for *m*-dinitrobenzene/NaY, while only the Na(II) sites are occupied for *m*-nitroaniline/NaY.[26] The presence of two sufficiently electronegative groups/atoms in one molecule at suitable distances appears to be one factor that is important in stabilizing the Na(III′) site in Y zeolites. Additional structural studies are now in progress, to determine the binding sites for a wider range of halocarbons and to allow a fuller understanding of the factors that govern halocarbon binding and cation migrations.

(23) Rubio, J. A.; Soria, J.; Cano, F. H. *J. Colloid Interface Sci.* **1980**, *73*, 312.

(24) Mortier, W. J.; Van den Bossche, E.; Uytterhoeven, J. B. *Zeolites* **1984**, *4*, 41.

(25) Kirschhock, C.; Fuess, H. *Stud. Surf. Sci. Catal.* (Weitkamp, J., Karge, H. G., Pfeifer, H., Hölderich, W., Eds.) **1994**, *84*, 843. Kirschhock, C.; Fuess, H. *Zeolites* **1996**, *17*, 388.

(26) Klein, H.; Kirschhock, C.; Fuess, H. *J. Phys. Chem.* **1994**, *98*, 12345.

Conclusions

The NMR and diffraction results presented in this paper have demonstrated that zeolite NaY cannot be considered an inert material under the conditions used for HFC-134/134a separations, and considerable rearrangement of extraframework cations occurs. Furthermore, this work potentially has significantly wider implications, since it suggests that similar structural rearrangements may be occurring in a wider range of adsorptions of similar molecules. Of particular relevance, for example, are the zeolitic systems that are effective for other HFC/HCFC/CFC separations, and as traps for halocarbon pollutants present in industrial wastes. We are now applying similar NMR and diffraction techniques to study a variety of systems, to assess how widespread this phenomenon is. Finally, this work has shown that the combination of NMR and diffraction techniques provides an effective method for studying adsorbent/adsorbate interactions, particularly when high degrees of order are not expected.

Acknowledgment. Continued stimulating conversations with M. Crawford are gratefully acknowledged. A. Wilkinson and A. L. Myers are thanked for their helpful comments concerning the data refinements and gas adsorptions, respectively. C. P. Grey and F. I. Poshni thank the NSF for partial support of this project through the National Young Investigator program (DMR-9458017) and for a grant (CHE-9405436) to purchase the NMR spectrometer. The financial support of DuPont, through an Aid to Education Award, and the U.S. Department of Energy, Office of Basic Energy Sciences (DE-AC 02-76CH00016), is acknowledged.

JA963565X